Global Journal of Engineering and Technology Advances

eISSN: 2582-5003

Cross Ref DOI: 10.30574/gjeta

Journal homepage: https://gjeta.com/

(Research Article)

Check for updates

# Study of the effects of annealing temperature on the properties of CuO/NiO thin films grown by Physical Vapor Deposition (PVD) technique for photovoltaic applications

ABDULRAHMAN RASHID HAMMOOD * and N.K. Hassan

*Education college for pure science, physics department, University of Tikrit, Iraq.*

Global Journal of Engineering and Technology Advances, 2023, 14(03), 076–083

Publication history: Received on 30 January 2023; revised on 11 March 2023; accepted on 14 March 2023

Article DOI: https://doi.org/10.30574/gjeta.2023.14.3.0049

## Abstract

Copper oxide/nickel oxide (CuO/NiO) thin films were deposited on glass substrates by the Physical vapor deposition (PVD) Technique and then annealed at different temperatures of 280°C, 320°C, and 360°C for 2 hours. The effects of the annealing temperature on the optical and structural properties of the CuO/NiO thin films were studied. X-ray diffraction suggests that a Monoclinic and cubic structure with a strong (1 1 1) and (2 2 0) for each of CuO and NiO respectively preferred orientation which remained the same with different heat treatments. And the crystallite size increases with annealing temperature, and the lattice constants of CuO/NiO thin films were also obtained from XRD data. Also, it is found that with the increase of different heat treatments, the optical absorption spectra showed that with increasing annealing temperatures, the absorption coefficient decreases, and the edge absorption shifts to longer wavelengths. The direct optical band gap decreases from 2.88 eV, 2.84ev to 2.74 eV for as-deposited and annealed CuO/NiO thin film at 280 °C, 320 °C, and 360 °C respectively.

**Keywords:** Nickel oxide; Annealing temperature; Physical vapor deposition; Thin film; Copper oxide

## 1. Introduction

The challenge for photoelectric researchers and manufacturers was to develop lower-cost, higher-efficiency devices.[1] However, typical Si photovoltaics with low defect wafers are very expensive and sophisticated processing processes such as wet chemical treatment, high-temperature furnace stages, and time-cost metallization. Significant efforts have recently been made to build low-cost photoelectric devices employing thin-film technology combined with the heterojunction principle. The interface between any two solid-state materials with diverse structural and optical properties is more frequently referred to as a heterojunction. The device junction in most heterojunction solar cells is created between TCO and Si or metal and Si.[2] TCOs that are commonly utilized are all n-type doped. Indeed, one of the major problems in the research is to create fresh p-type TCOs with comparable performance to their n-type counterparts. Although several p-type materials (such as CuO and NiO) [3] [4] have been proposed, their material characteristics are still subpar when compared to n-type TCOs. To create p heterojunctions and create a variety of new devices, a high mobility/conductivity p-type TCO might be combined with well-known n-type TCOs. This would open new possibilities for transparent electronics. Furthermore, p-type TCOs would find use in thin-film transistors,[5] as efficient hole-transport layers in solar cell systems[6]or in dye-sensitized solar cells [6] [7] Both practical and theoretical data about the electrical structure of metal oxides should be taken into consideration for the optimum design of p-type TCOs.[4], [8], [9] To encourage the creation of highly hybridized orbitals that boost the VBM level and make hole doping easier, metals with d orbitals near to the O 2p can be employed. Cu2O is a strong contender in this regard since the O 2p6 and Cu+'s 3d10 arrangement are quite similar. Additionally, it produces shallow and effective holes due to the production of copper vacancies (VCu), which makes it fundamentally copper-deficient [10]. The 3d8 configuration of Ni2+ is also suitable for obtaining p-type NiO, with an easy hole dupability by cation deficiency [11] Due to its hole dupability (p-type behavior), which is assumed to be caused by the nonstoichiometric of NiO, NiO has been one of the

* Corresponding author: ABDULRAHMAN RASHID HAMMOOD

most researched wide-gap oxides (cation deficiency) [11], The transparency (Eg = 3.7eV) and p-type behavior of this material [12] manufacture transparent conductor oxide (TCO) with applications in smart windows out of NiO, a promising substance [13] and photovoltaics [14].

## 2. Experimental Details

### 2.1. Sample preparation

Glass slides measuring (76x21x1) millimeters were employed as the substrate in this experiment for the deposition of CuO/NiO thin films, after being cleaned with ethanol and distilled water, dried, and cleaned with optical cleaning paper. CuO/NiO films were created utilizing the physical vapor deposition process, as demonstrated in (Fig. 1), using copper and nickel powders with a purity level of 99.9 percent. The material that will be deposited on the substrates will be vaporized as part of the CuO/NiO thin layer manufacture process under low pressure up to 10-6 m bar. The substrate was 20 cm away from the target.

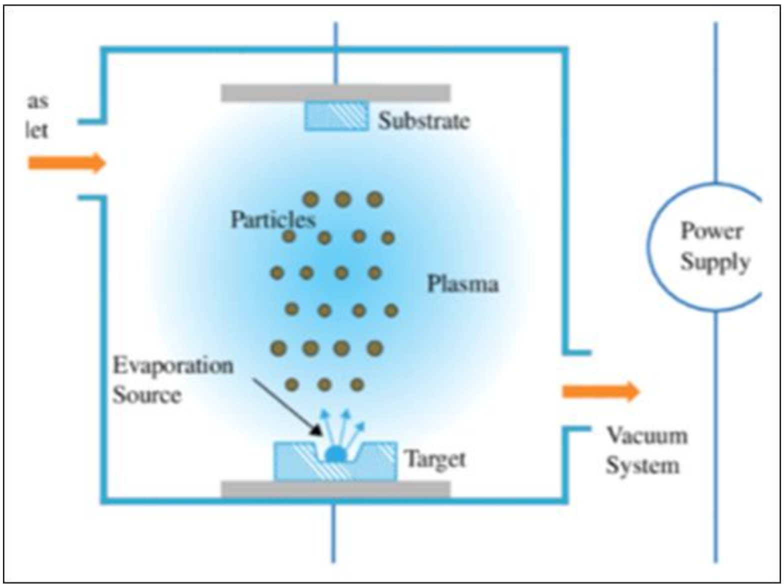


**Figure 1** Schematic-illustration-of-physical-vapor-deposition-PVD-process

## 3. Results and discussion

### 3.1. Structure and morphology of the CuO/NiO films

By comparing the results of the X-ray diffraction measurement to the ASTM (American Society of Testing Materials) cards, can we determine the growth films' nature and the structural characteristics of CuO/NiO films.) (Figure 3) illustrates the x-ray diffraction patterns of CuO/NIO thin films that were annealed at various temperatures for the same period. at 280 °C XRD peaks obtained show that films have a polycrystalline structure with single-phase Cu2O as a cubic structure at diffraction angles of 29.582, 36.46, 42.20, 52.51, 61.06, 69.08, 73.66, and 77.24, corresponding to the crystal planes (1 1 0), ( 1 1 1), ( 2 0 0), (2 1 1 ), (2 2 0 ), (3 1 0 ), ( 3 1 1) and (2 2 2 )and NiO with cubic structure at diffraction angles of 37.360, 43.478, and 62.845 corresponding to the planes ( 1 1 1) , (2 0 0 ) and (2 2 0 ) and the films annealed at 320 ∘C have a Monoclinic structure with single-phase Tenorite CuO at diffraction angles of 35.125, 38.51, 49.54, 53.05, 58.65, and 61.379, which corresponding to (-1 1 1 ), ( 1 1 1) (-2 0 2 ), (0 2 0) (2 0 2 ) and ( -1 1 3) In particular, the film annealed at less than 300 °C has a two-phase mixed polycrystalline structure containing Cu2O and CuO phases. Obviously, 300 ∘C is the phase-transition temperature at which the Cu2O film is transformed into a CuO film by thermal annealing. In addition, from the XRD pattern of the Cu2O-CuO mixed film, it can be clearly observed that the intensities of the Cu2O XRD-peaks are very weak (almost disappearing), indicating that the film is mainly composed of CuO and contains a small amount of Cu2O, as well as peaks of nickel oxide (NiO), at diffraction angles of 37.852, 43.44, and 63.19, which corresponding to planes (1 1 1 ), (2 0 0 ) and (2 2 0 ) with a cubic structure at an annealing temperature of 360 °C we obtained on ten peaks of Tenorite CuO at diffraction angles of 32.13, 35.25, 38.51, 46.17, 48.63, 51.23, 53.32, 58.26, 61.23, 72.16, and 73.07 corresponding to (1 1 0 ) , (-1 1 1 ) , (1 1 1 ) , (-1 1 2 ) , (-2 0 2 ) , (1 1 2 ), (0 2 0 ) , ( 2 0 2) , (-1 1 3 ) , ( 3 1 1) and (2 2 1 ) with

Monoclinic structure and pattern of Bunsenite NiO at diffraction angles 37.46, 43.44, 63.19, 75.40 and 79.31 corresponding to (1 1 1 ), (2 0 0 ) , (2 2 0 ) , (3 1 1 ) and (2 2 2 ) with cubic structure with an increase in the intensity of the copper oxide peaks (CuO) in a preferred direction (1 1 1) corresponding to the diffraction angle (38.6363) with COD File (No. 01-078-0428) and intensity of the nickel oxide peaks in a preferred direction (2 2 0) corresponding to the diffraction angle (63.1976) with COD File (No. 00-001-1239.) Also, the intensity of the peaks increases with the increase in the annealing temperature. An increase in the number of peaks for copper oxide and nickel oxide and their intensity at certain crystalline levels with an increase in the annealing temperature indicates an increase in the crystallinity of the material and the regularity of its crystalline structure, which gives a greater opportunity for constructive interference to occur because of achieving the Bragg condition for diffraction.

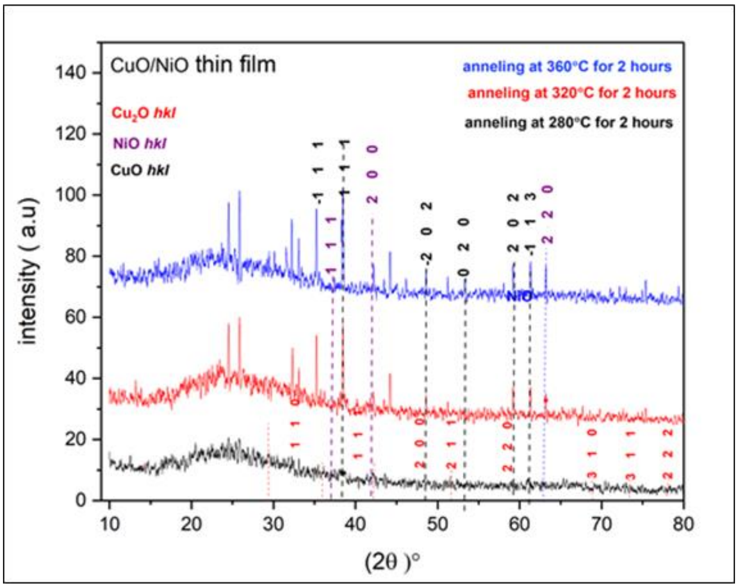


**Figure 2 A** comparison between the x-ray diffraction patterns of CuO/NIO thin films annealed at different temperatures

The average grain size (GS) of the polycrystalline material can be calculated from the X–ray spectrum by means of the Full Width at Half Maximum (FWHM) method (Scherrer relation). [15,16] (equation 1), shows an increase in the particle size with the temperature and agrees with the sizes measured by the scanning electron microscope also Micro strain (ε) and Dislocation Density (δ) calculated by (equation 2 and equation 3) as shown in (table 1). By using (equation.4), the lattice constants and Miller indices were calculated, and they agreed with the measurements taken from the JCPDS card as shown in (table .2)

$$D = \frac{k\lambda}{\beta\,(2\theta)\cos\theta} \quad \text{.......................}(1)$$

β is the full–width at half maximum of the XRD peak appearing at the diffraction angle θ, k the shape factor, the value of which depends on the crystalline shape, and generally it is 1.

The micro-strain (ε) and the dislocation density ($\delta$) of the films are estimated using the following formula. [17], [18]:

$$\varepsilon = \frac{\beta\cos\theta}{4} \quad \text{.......................}(2)$$

$$\delta = \frac{1}{D^2} \quad \text{..................}(3)$$

The lattice constants a, b, and c of the CuO/NiO structure were calculated, according to Bragg's law [19]

$$2d\,\sin\theta = n\lambda \quad \text{....................}(4)$$

**Table 1** The particle size D, Micro strain (ε) and Dislocation Density (δ) with the annealing temperature

| **Annealing temperatures** | **Parameters** | | **Peak position** | **FWHM** | **D (nm)** | **Micro strain (ε)** | **Dislocation Density (δ)** |
|---|---|---|---|---|---|---|---|
| | K | λ (Å) | 2θ (°) | β (°) | | x10-3 | x10-4 |
| 280 ºC | 0.94 | 1.5406 | 38.152 | 0.208 | 42.16 | 2.62 | 5.63 |
| 320 ºC | 0.94 | 1.5406 | 38.461 | 0.171 | 51.34 | 2.14 | 3.79 |
| 360 ºC | 0.94 | 1.5406 | 38.581 | 0.054 | 162.79 | 0.75 | 0.46 |

**Table 2** The lattice constants a, b, and c, miller indices with the measurements taken from the JCPDS card

| **Annealing temperatures** | **sample** | ***2θ (deg.)*** | ***d(Å)*** | ***Lattice constant (Å)*** | ***Lattice constant (Å)* JCPDS** | ***Miller indices hkl*** |
|---|---|---|---|---|---|---|
| **280 ºC** | $Cu_2O$ | 29.4089 | 3.0347 | a=4.2917 | a=4.2520 | 110 |
| | | 36.1518 | 2.4826 | b=4.3000 | b=4.2520 | 111 |
| | | 42.8253 | 2.1099 | c=4.2199 | c=4.2520 | 200 |
| | NiO | 37.6007 | 2.3902 | a=4.1400 | a=4.1760 | 111 |
| | | 42.8257 | 2.1099 | b=4.2198 | b=4.1760 | 200 |
| | | 62.4457 | 1.4860 | c=4.2031 | c=4.1760 | 220 |
| **320 ºC** | CuO | 38.6363 | 2.3285 | a=4.0331 | a=4.6530 | 111 |
| | | 32.5235 | 2.7508 | b=3.8902 | b=3.4100 | 110 |
| | | 49.68654 | 1.8334 | c=5.1858 | C=5.1080 | -202 |
| | NiO | 37.3354 | 2.4066 | a=4.1683 | a=4. 1684 | 111 |
| | | 43.4483 | 2.0811 | b=4.1622 | b=4. 1684 | 200 |
| | | 63.1976 | 1.4701 | c=4.1582 | c=4. 1684 | 220 |
| **360 ºC** | CuO | 38.46083 | 2.3387 | a=4.0508 | a=4.6530 | 111 |
| | | 32.23791 | 2.7745 | b=3.9238 | b=3.4100 | -110 |
| | | 35.23946 | 2.5448 | C= 5.0896 | C=5.1080 | 002 |
| | NiO | 43.1208 | 2.0962 | a=4.1923 | a=4.1710 | 200 |
| | | 63.0565 | 1.4731 | b=4.1665 | b=4.1710 | 220 |
| | | 75.4076 | 1.2595 | c=4.1774 | c=4.1710 | 311 |

The morphology of the films was characterized using SEM at a 10 keV operating voltage (Fig.3) shows typical SEM images of CuO/NiO nanocomposite thin films grown on glass substrates with varying annealing temperatures. The findings demonstrated that the CuO/NiO thin layer has a fine nanoparticle structure and is prone to aggregate because of the homogeneity of the nanoparticles' surfaces and their high surface energy and surface tension. and is evenly diffused across all substrates. With The CuO/NiO films' grain size increasing with annealing temperature, as seen in (Fig.3 a, b, and c), Continuous grain distribution shows that the grains cling properly to the prepared films' surface.

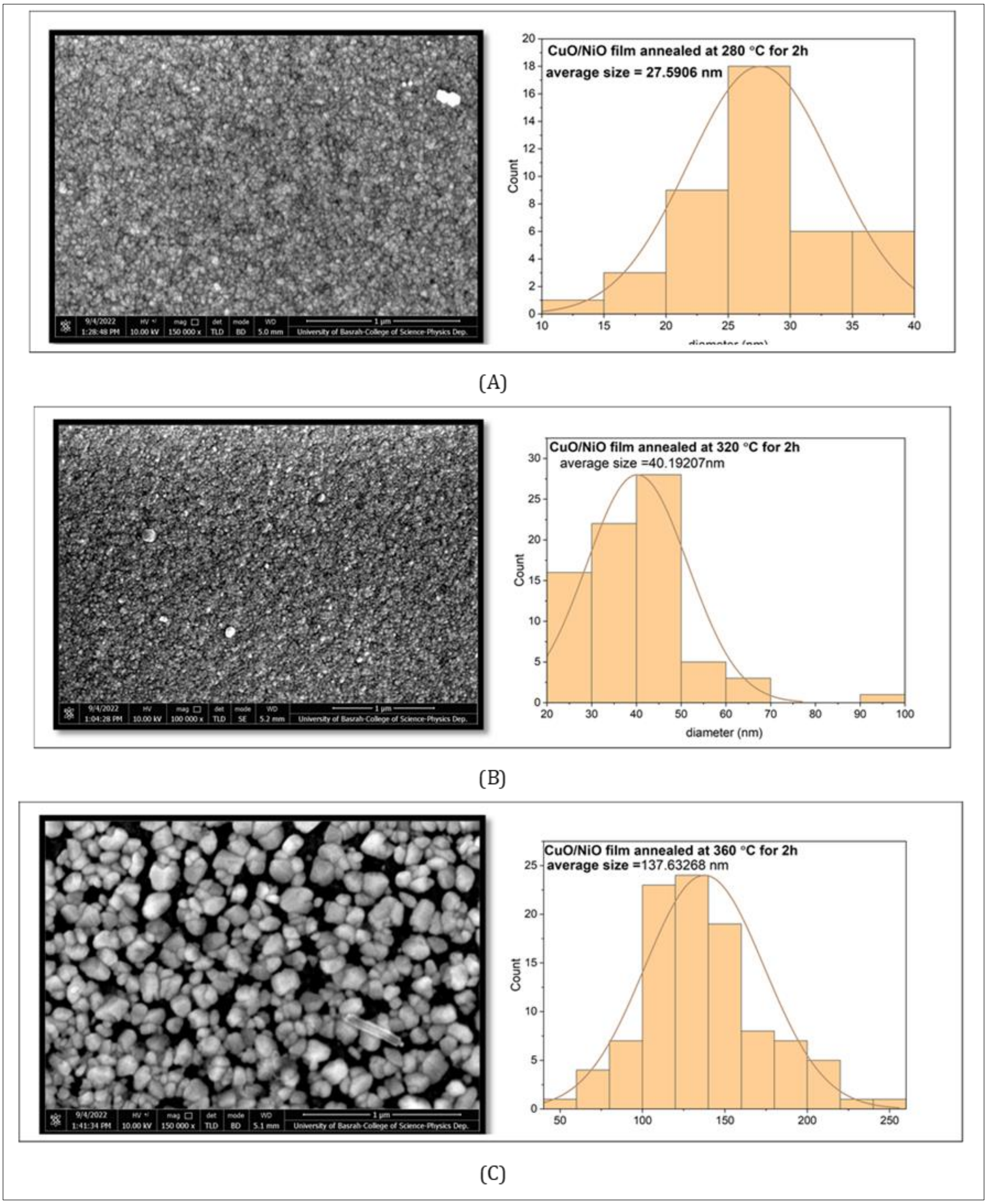


**Figure 3** SEM images of the CuO/NiO nanocomposite thin films grown on glass substrates under various annealing temperatures

### 3.2. Optical properties

Optical transmission spectra depend on the chemical and crystal structure of the films, the film thickness, and on film's surface morphology. The effect of different annealing temperatures on the transparency is increasing with increasing annealing temperature due to decreasing in the thickness of the film with increasing annealing temperature The crystallization of thin films strongly depends on the annealing temperature. At higher temperatures, films have fewer impurities, and it is the origin of varying electrical and optical properties. In the direct band gap structure or direct transition semiconductors (present case), the absorption coefficient and optical band gap (Eg) are related by [20].

$$\boldsymbol{\alpha} = (\,\boldsymbol{hv} - \boldsymbol{Eg})^{1/2} \quad \text{……………..(5)}$$

h is Plank's constant and υ is the frequency of the incident photon

The optical properties of deposited CuO/NiO film on glass substrate at various annealing temperatures of (280,320, and 360) C. The optical transmittance is at normal incidence in the wavelength range (300-1100) nm. Shows the (UV–Visible) absorption spectra of as-prepared and annealed CuO/NiO samples at different temperatures. The absorption peak for as prepared CuO/NiO sample is observed around 350 nm. However, A clear decrease in absorbance is observed with increasing wavelength for the CuO/NiO products annealed at between (350-550) nm, which may be due to a change in crystallite size. we can observe that (fig. 4) shows absorption as a function of wavelength, where absorption decrease with increasing temperature, which may be due to a change in crystallite size.

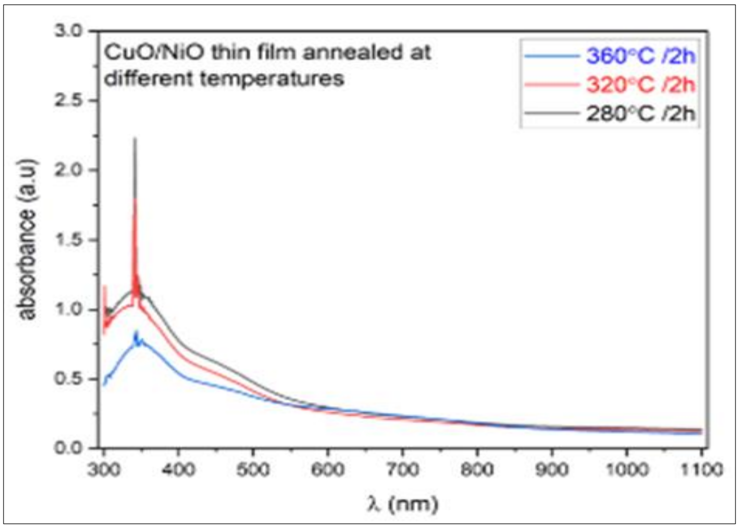


**Figure 4** The relationship between absorbance as a function of wavelength of CuO/NiO films annealed at 280°C/2h ,320°C/2h, and 360°C/2h

By using equation (5) The optical energy gap (Eg) value is calculated by extrapolation of the straight line of the plot of $(\alpha h\upsilon)^2$ versus photon energy for different annealing temperatures as shown inset in (Fig.5) The linear dependence of $(\alpha h\upsilon)^2$ with (hυ) indicates direct band gap. The annealed samples show a relative decrease in optical band gap with annealing temperature. The films as deposited and annealed at 280 °C have a band gap of about 2.88 eV and at 320 °C has 2.84 eV. And at 360 °C annealed films, the optical band gap continues to decrease close to 2.71 eV.

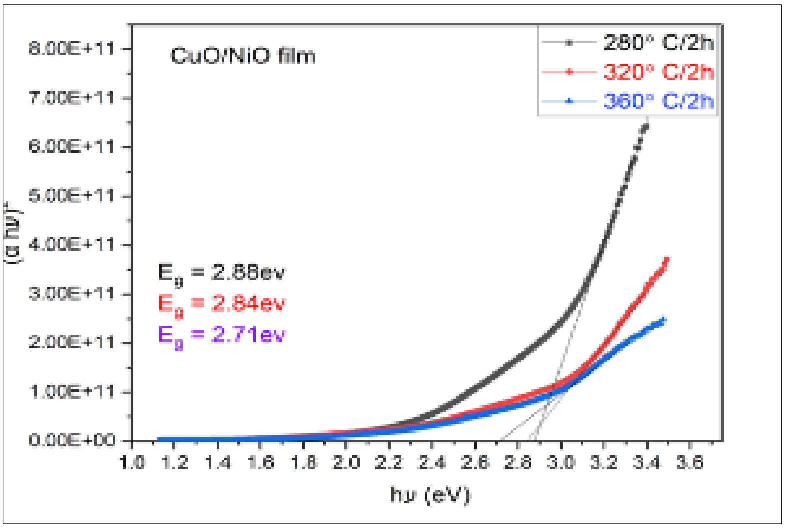


**Figure 5** Tauc plots of the CuO/NiO thin film annealing at different temperatures

## 4. Conclusion

An efficient, simpler, and cheaper PVD technique successfully employed in depositing nanocrystalline CuO/NiO thin films on a glass substrate. The prepared films have uniform morphology and are tightly adherent to the substrate. The XRD results showed that the intensity and crystallite size increase with increasing annealing temperature. The morphological results showed that the grains are well distributed over the substrate and the films have high homogeneity. Also, the optical energy gap was found to be decreased with increase annealing temperature (Eg= 2.88, 2.84, and 2.71) eV for annealing temperature (280, 320, and 360) respectively. The high transparency and wide band gap features make these films to be suitable in nano-optoelectronic applications, especially in the solar cell as a window or antireflection layer.

## Compliance with ethical standards

### *Acknowledgments*

First of all, I would like to extend my thanks and appreciation to the Presidency of Tikrit University and the Deanship of the College of Education for Pure Sciences, especially my supervisor, Professor Dr. Nadim Khaled Hassan. I also thank everyone who contributed to the completion of my work.

### *Disclosure of conflict of interest*

We did this work with my supervisor, Dr. Nadim Khaled Hassan, because there is a common interest, which is the scientific promotion in our university, and there is no conflict of interest between us If you have questions or concerns about my financial interests as they relate to this research, please let me know.  If you have questions or concerns about data integrity or research participant safety at any time because of this conflict of interest, you may contact [dr. Nadim Khalid Hassan] or the Tikrit University Conflict of Interest Office.

## References

[1] M. M. D. Kumar, J. H. Yun, and J. Kim, “Metal/semiconductor and transparent conductor/semiconductor heterojunctions in high efficient photoelectric devices: Progress and features,” International Journal of Photoenergy, vol. 2014. Hindawi Publishing Corporation, 2014. doi: 10.1155/2014/160379.

[2] G. N. Lee, M. Ponnamma Machaiah, W. H. Park, and J. Kim, “Enhanced Optical and Electrical Properties of ITO/Ag/AZO Transparent Conductors for Photoelectric Applications,” International Journal of Photoenergy, vol. 2017, 2017, doi: 10.1155/2017/8315802.

[3] K. H. L. Zhang, K. Xi, M. G. Blamire, and R. G. Egdell, “P-type transparent conducting oxides,” Journal of Physics Condensed Matter, vol. 28, no. 38. Institute of Physics Publishing, Jul. 27, 2016. doi: 10.1088/0953-8984/28/38/383002.

[4] Z. Wang, P. K. Nayak, J. A. Caraveo-Frescas, and H. N. Alshareef, “Recent Developments in p-Type Oxide Semiconductor Materials and Devices,” Advanced Materials, vol. 28, no. 20. Wiley-VCH Verlag, pp. 3831–3892, May 25, 2016. doi: 10.1002/adma.201503080.

[5] E. Fortunato, P. Barquinha, and R. Martins, “Oxide semiconductor thin-film transistors: A review of recent advances,” Advanced Materials, vol. 24, no. 22. pp. 2945–2986, Jun. 12, 2012. doi: 10.1002/adma.201103228.

[6] J. Bandara and J. P. Yasomanee, “P-type oxide semiconductors as hole collectors in dye-sensitized solid-state solar cells,” Semicond Sci Technol, vol. 22, no. 2, pp. 20–24, Feb. 2007, doi: 10.1088/0268-1242/22/2/004.

[7] C. S. Chou, C. M. Hsiung, C. P. Wang, R. Y. Yang, and M. G. Guo, “Preparation of a counter electrode with p -type nio and its applications in dye-sensitized solar cell,” International Journal of Photoenergy, vol. 2010, 2010, doi: 10.1155/2010/902385.

[8] G. Hautier, A. Miglio, G. Ceder, G. M. Rignanese, and X. Gonze, “Identification and design principles of low hole effective mass p-type transparent conducting oxides,” Nat Commun, vol. 4, 2013, doi: 10.1038/ncomms3292.

[9] R. Cao, H. X. Deng, and J. W. Luo, “Design Principles of p-Type Transparent Conductive Materials,” ACS Applied Materials and Interfaces, vol. 11, no. 28. American Chemical Society, pp. 24837–24849, Jul. 17, 2019. doi: 10.1021/acsami.9b01255.

[10] H. Raebiger, S. Lany, and A. Zunger, "Origins of the p-type nature and cation deficiency in Cu2 O and related materials," Phys Rev B Condens Matter Mater Phys, vol. 76, no. 4, Jul. 2007, doi: 10.1103/PhysRevB.76.045209.

[11] J. Osorio-Guillén, S. Lany, and A. Zunger, "Nonstoichiometry and hole doping in NiO," in AIP Conference Proceedings, 2009, vol. 1199, pp. 128–129. doi: 10.1063/1.3295330.

[12] Z. Zhang, Y. Zhao, and M. Zhu, "NiO films consisting of vertically aligned cone-shaped NiO rods," Appl Phys Lett, vol. 88, no. 3, pp. 1–3, 2006, doi: 10.1063/1.2166479.

[13] G. A. Niklasson and C. G. Granqvist, "Electrochromics for smart windows: Thin films of tungsten oxide and nickel oxide, and devices based on these," J Mater Chem, vol. 17, no. 2, pp. 127–156, 2007, doi: 10.1039/b612174h.

[14] M. D. Irwin, D. B. Buchholz, A. W. Hains, R. P. H. Chang, and T. J. Marks, "p-Type semiconducting nickel oxide as an efficiency-enhancing anode interfacial layer in polymer bulk-heterojunction solar cells," 2008. [Online]. Available: www.pnas.org/cgi/content/full/

[15] N. K. Hassan, M. R. Hashim, and N. K. Allam, "A facile room temperature electrochemical deposition of pyramidal ZnO nanostructures: Suppressing the green emission," Physica E Low Dimens Syst Nanostruct, vol. 44, no. 9, pp. 1853–1856, Jun. 2012, doi: 10.1016/j.physe.2012.05.006.

[16] B.D. Cullity &S.R. Stock, Elements of X-Ray Diffraction. 2011. [Online]. Available: www.iran-mavad.com

[17] M. N. A. A. K. Salim, "Influence of Doping Concentration on the Properties of Tin Doped Zinc Oxide Thin Films Prepared by Spray Pyrolysis for Photovoltaic Applications," International Journal of Thin Film Science and Technology, vol. 10, no. 3, pp. 197–204, Sep. 2021, doi: 10.18576/ijtfst/100309.

[18] M. N. Amroun, K. Salim, and A. H. Kacha, "Molarities effect on structural optical and electrical properties of nanostructured zinc oxide deposited by spray pyrolysis technique," International Journal of Thin Film Science and Technology, vol. 10, no. 1, pp. 67–73, 2021, doi: 10.18576/ijtfst/100110.

[19] F. K. Shan et al., "Blueshift of near band edge emission in Mg doped ZnO thin films and aging," J Appl Phys, vol. 95, no. 9, pp. 4772–4776, May 2004, doi: 10.1063/1.1690091.

[20] J. F. Mohammad, M. A. A. Sooud, and S. M. Abed, "CHARACTERISTICS OF pH VARIATION ON STRUCTURAL AND OPTICAL PROPERTIES OF NANOCRYSTALLINE SnO 2 THIN FILMS BY CBD TECHNIQUE."